Sum-frequency generation in disordered quadratic nonlinear media

Fabian Sibbers, Jörg Imbrock*, and Cornelia Denz

Institut für Angewandte Physik and Center for Nonlinear Science (CeNoS),
Westfälische Wilhelms-Universität Münster, 48149 Münster, Germany

ABSTRACT

We study the process of sum-frequency generation of femtosecond laser pulses in a strontium barium niobate crystal with a random distribution of ferroelectric domains. The random domain structure allows for broadband quasi-phase matching of wavelengths over the whole visible spectrum. We analyze sum-frequency generation in the wavelength range 460 nm − 630 nm, which is emitted on a cone with angles between 30 ° and 55 °. We measure the effective angular width of the sum-frequency intensity profile which is related to the spectral pulse width and directly visualizes the spectral pulse broadening due to self-phase modulation.

Keywords: sum-frequency generation, random media, SBN

1. INTRODUCTION

Three-wave mixing processes such as sum-frequency generation (SFG), second-harmonic generation (SHG), and difference-frequency generation belong to the best studied optical nonlinear effects. The efficiency of the generation of new optical frequencies depends critically on the matching of the phase velocities of the interacting waves. The most versatile technique for quasi-phase matching is to periodically pole ferroelectric crystals, where the phase mismatch is compensated for by a reciprocal grating vector.[1] This concept can be extended to a two-dimensional (2D) modulation of the quadratic nonlinearity.[2] However, the discrete modulation of the nonlinearity just allows for the phase matching of a discrete set of wavelengths. Broadband parametric processes can be realized in media with a disordered structure of the nonlinearity like in polycrystalline ferroelectrics[3] and in ferroelectric crystals with randomly distributed antiparallel microdomains like calcium barium niobate (CBN),[4] strontium tetra borate (SBO),[5] and strontium barium niobate (SBN).[6] The random domain structure of SBN allows for broadband quasi-phase matching of wavelengths over the whole visible spectrum. Due to the noncollinear phase-matching condition the signal of the second harmonic is emitted either in a plane,[6,7] on a cone[7–10] or in form of a toroid.[11] It has also been demonstrated that noncollinear second-harmonic generation in SBN can be used to characterize femtosecond laser pulses.[12–14] As the angular spectrum of planar SHG is directly related to the domain distribution this process can be used for k-spectroscopy[15,16] and to examine the switching behavior of ferroelectric domains.[17–19] Aside from noncollinear SHG the generation of the third harmonic via a cascaded $\chi^{(2)}$-process is also possible.[10,20] However, up to now *noncollinear sum-frequency generation* in SBN is not well examined. Emission of green (SHG) and blue (SFG) light has been observed when an SBN crystal was placed inside a laser cavity,[21,22] but this sum-frequency emission was measured just at one fixed wavelength and only in the planar geometry. Most of the published results concerning noncollinear SHG in SBN have been achieved either with ultrashort laser pulses of relatively low pulse energy or with longer pulses in the picosecond and nanosecond regime. Therefore, not much is known about noncollinear frequency conversion of high energy ultrashort laser pulses. Propagation of high energy pulses can lead to additional nonlinear effects like self-phase modulation which can be studied by analyzing the conical second-harmonic emission.

In this paper we study conical SFG of high energy ultrashort laser pulses in SBN with a random structure of ferroelectric domains. The angular distributions of the second-harmonic (SH) and sum-frequency (SF) intensities are measured and compared with theory. We study how the width of the second-harmonic intensity profile depends on the spectral pulse width, which broadens with increasing pulse energy.

* imbrock@uni-muenster.de

Nonlinear Optics and Applications IV, edited by Benjamin J. Eggleton, Alexander Luis Gaeta, Neil G. R. Broderick
Proc. of SPIE Vol. 7728, 77280Y · © 2010 SPIE · CCC code: 0277-786X/10/$18 · doi: 10.1117/12.855885

2. DOMAIN-INDUCED FREQUENCY CONVERSION

In this section we give an overview of different noncollinear phase matching schemes for domain-induced frequency conversion in SBN. The crystal used is undoped $Sr_xBa_{1-x}Nb_2O_6$ with the congruently melting composition ($x = 0.61$). All surfaces are polished to optical quality and the dimensions are $5 \times 5 \times 5\,\mathrm{mm}^3$. The z-axis corresponds to the c-axis, which is oriented parallel to one crystal edge. A random domain structure is induced by heating the crystal above the Curie temperature ($T_C \approx 70\,^\circ\mathrm{C}$) to $200\,^\circ\mathrm{C}$ into the paraelectric phase followed by a cooling-down into the ferroelectric phase. The crystal shows a disordered structure of $180\,^\circ$ needle-like domains at room temperature. The domains have a round shape, are tens of micrometers long, and the diameter varies between 100 nm and a few micrometers,[15] while the mean diameter is about $2.5\,\mu$m.[10] All experiments are carried out with the same crystal.

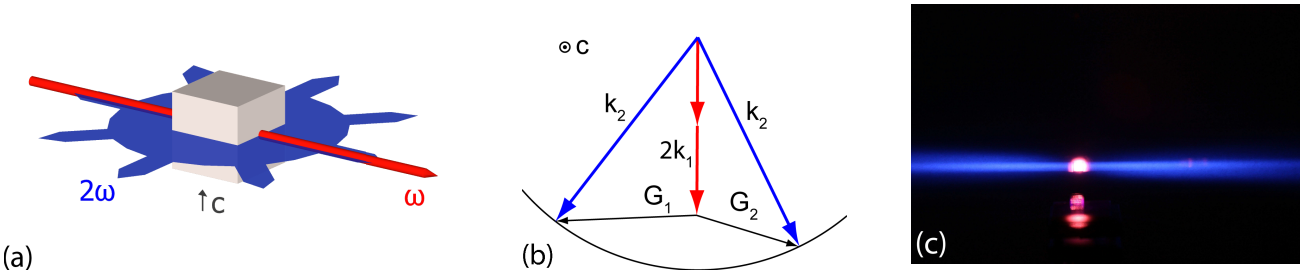

Figure 1. (Color online) Planar SHG. (a): SH emission in a plane perpendicular to c-axis; (b): phase matching condition; (c): photograph of 400 nm emission (SH of 800 nm).

As the $\chi^{(2)}$ nonlinearity is randomly modulated in two dimensions the crystal can be regarded as a 2D nonlinear photonic crystal. The random domain structure provides a large set of grating vectors $\mathbf{G}$ for quasi-phase matching: $\mathbf{k}_1 + \mathbf{k}_2 + \mathbf{G} = \mathbf{k}_3$, where $\mathbf{k}_1$ and $\mathbf{k}_2$ denote the wave vectors of the fundamental waves and $\mathbf{k}_3$ is the wave vector of the SHG and SFG wave, respectively. Without these random domains no exact phase matching for SHG in the visible spectrum would be possible, because of the small birefringence of SBN.[23]

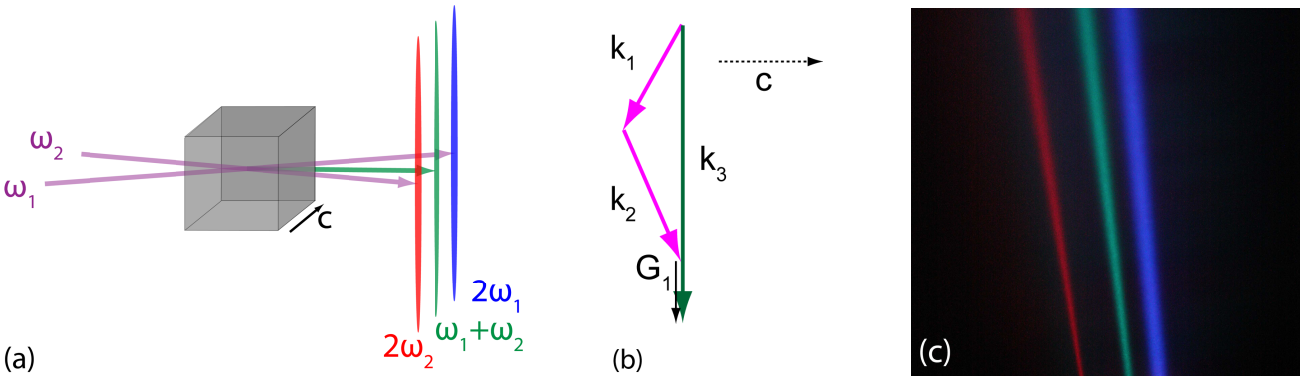

Figure 2. (Color online) quasi-collinear SFG. (a): SFG and SHG emissions in planes perpendicular to c-axis; (b): phase matching condition; (c): photograph of 650 nm emission (SH of 1300 nm), 495 nm emission (SFG of 800 nm and 1300 nm), and 400 nm emission (SH of 800 nm).

Ultrashort laser pulses are generated by a laser system consisting of a mode-locked Ti:sapphire oscillator, a regenerative amplifier and an optical parametric amplifier. The repetition rate is 1 kHz, the pulse duration is about $\tau_p = 80$ fs, the spatial pulse diameter is $w = 2.5$ mm, and the pulse energies are up to $100\,\mu$J depending on the wavelength which can be tuned between 470 nm and 2900 nm. The signal waves ($1.1\,\mu$m - $1.6\,\mu$m) of the parametric amplifier are perpendicular polarized to the idler waves ($1.6\,\mu$m - $2.9\,\mu$m), and the pump wave (800 nm) is polarized parallel to the idler waves. To study the conical SH emission we have used the signal and

idler waves. For the SFG experiments the pump pulses at 800 nm are used together with the signal and idler waves.

When a laser pulse of frequency ω_1 propagates perpendicular to the c-axis of the crystal, a second harmonic signal ($2\omega_1$) and sometimes a third harmonic signal ($3\omega_1$) are generated in a plane perpendicular to the c-axis. In Fig. 1 the SH emission (a) and the phase matching condition (b) are illustrated. The photograph (Fig. 1(c)) shows the SH emission at 400 nm. To study SF mixing processes it is more practical to use a geometry, where all generated frequencies are not located in the same plane. For example a quasi-collinear pulse superposition[13,24] generates SH and SF signals in different planes (Fig. 2). The photograph in Fig. 2(c) shows the red SH of 1300 nm (left), green SF of 800 nm and 1300 nm (middle), and the blue SH of 800 nm (right).

Not only a spatial separation of the second-harmonic and sum-frequency waves but also a spectral fanning of all generated waves can be realized by a pulse propagation along the c-axis.[8] In Fig. 3 an example for conical SH and SF emission is given. Fig. 3(c) shows the mixing of three waves with the wavelengths 800 nm, 1300 nm, and 2087 nm. We now assume that two laser pulses with frequencies ω_1 and ω_2 are propagating collinearly parallel

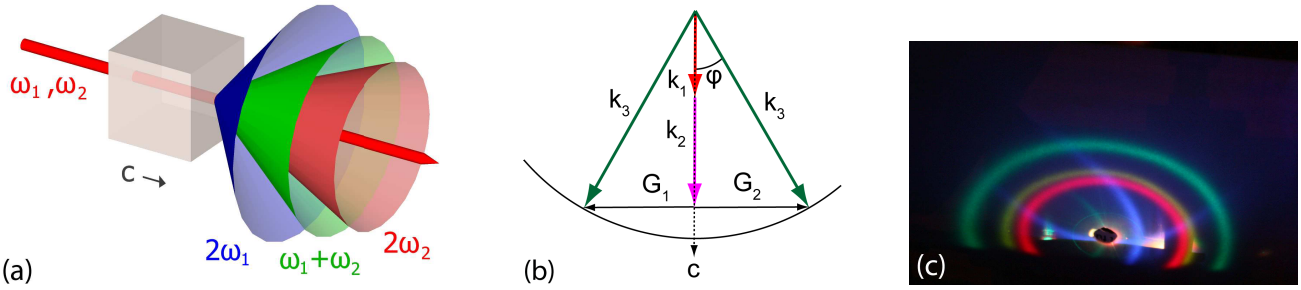

Figure 3. (Color online) Conical SFG. (a): SFG and SHG emissions on cone along c-axis; (b): phase matching condition; (c): photograph of conical wave mixing of three wavelengths: 800 nm, 1300 nm, and 2087 nm.

to the c-axis. To fulfill the phase matching condition (Fig. 3(b)), the SHG and SFG signals are emitted on a cone with the angle φ inside the crystal depending on the ordinary and extraordinary refractive indices n^{o} and n^{e} of the participating waves:

$$\cos\varphi = (k_1 + k_2)/k_3 = \left(\frac{n_1^{\mathrm{o}}}{\lambda_1} + \frac{n_2^{\mathrm{o}}}{\lambda_2}\right) / \left(\frac{n_3^{\mathrm{e}}(\varphi, \lambda_3)}{\lambda_3}\right) . \quad (1)$$

The angle Θ outside the crystal can be calculated with Snell's law. As the extraordinary refractive index n^{e} itself depends on the angle φ, Eq. 1 has to be solved numerically.

3. CONICAL SECOND-HARMONIC GENERATION AND SUM-FREQUENCY GENERATION

First, we demonstrate the process of conical SFG by mixing the wavelengths 800 nm, 1300 nm, and 2087 nm inside the crystal. Using a polarizer all waves are polarized 45 ° with respect to the x-axis. The generated conical emission can be seen on the photograph in Fig. 3(c). To analyze the different generated frequencies we have measured the spectrum of each ring (Fig. 4) with a spectrometer with a resolution of 0.2 nm. All expected visible frequencies can be found: 400 nm (SHG of 800 nm), 495 nm (SFG of 800 nm and 1300 nm), 578 nm (SFG of 800 nm and 2087 nm), and 650 nm (SHG of 1300 nm). The intensities of different wavelengths are not to scale, but it should be noted that the SHG of 1300 nm is much broader than the other generated frequencies.

The cone angle Θ, which belongs to the maximum intensity on the ring, was measured behind the crystal by projecting the emitted light onto a screen. Each ring has also an angular width of $\Delta\Theta$, which depends on the spectral pulse width (see section 5). The results for SHG and SFG are depicted in Fig. 5. For SFG λ_1 has been kept fixed at 800 nm and λ_2 was tuned continuously between 1.1 μm and 2.9 μm. The lines are calculations of Eq. 1 using the refractive indices of the Sellmeier equation,[23] which fit very well to the experimental data. Second-harmonic and sum-frequency pulses with wavelengths shorter than 408 nm experience total internal reflection.

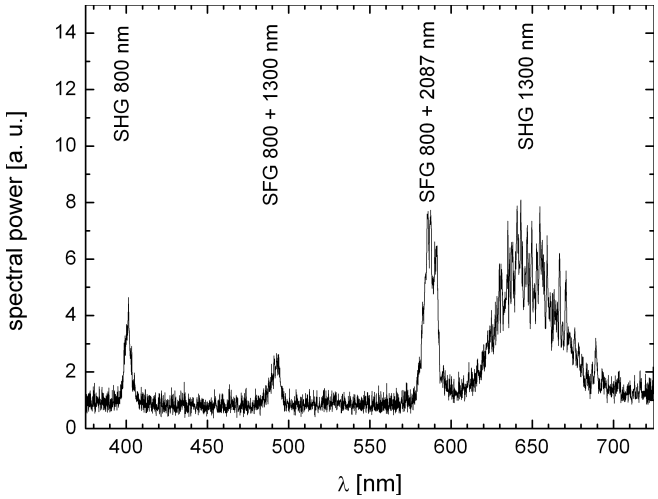

Figure 4. Spectrum of the generated pulses behind the crystal when three waves with the wavelengths 800 nm, 1300 nm, and 2087 nm are mixed inside the crystal (see Fig. 3(c)).

Hence, no 400 nm ring can be observed in the experiments. Instead, reflections of the 400 nm ring at the crystal sides appear inside the other rings (Fig. 3(c)). As each spectral component is emitted at a specific angle $\Theta(\lambda)$ over a large range, conical SHG and SFG can be considered as a *nonlinear superprism* effect. Our results of the SHG measurements agree very well with previously published results[10] and we also see no deviations in the angular spectrum due to thermal focusing, which can be observed with 820 nm fs laser pulses at high repetition rates of 80 MHz.[7,25] The SHG output power increases almost quadratically with increasing input power as expected for a $\chi^{(2)}$-process. An estimation of the conversion efficiency for frequency doubling of a 1200 nm pulse with an energy of 100 μJ yields 0.01 %. Comparing the wavelength sensitivity of the SHG and the SFG process, the SFG process shows a higher sensitivity in the red spectral range. As the angle Θ of the SF signal depends on both wavelengths λ_1 and λ_2, this process can in principle be used for all optical deflection, where one control pulse controls the deflection of a signal pulse.

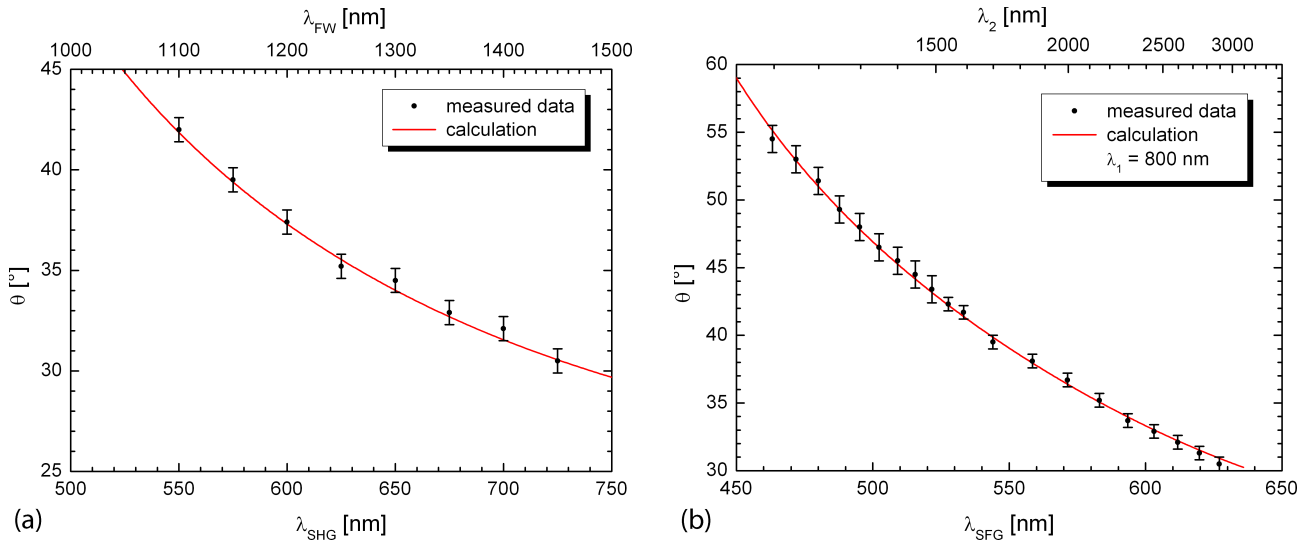

Figure 5. Cone angle Θ outside the crystal in dependence of generated wavelength for SHG (a) and SFG (b). The dots are measured values and the lines are calculations with Eq. 1.

4. POLARIZATION DEPENDENCE OF CONICAL SUM-FREQUENCY GENERATION

In the process of conical SFG the fundamental waves are propagating along the c-axis and therefore they are always ordinarily polarized, while the sum-frequency waves are radially polarized.[8] In the experiments presented so far, all fundamental waves were polarized parallel to each other, because no sum-frequency wave can be generated if the participating waves are polarized perpendicular to each other. This is illustrated in Fig. 6, where three waves with the wavelengths 800 nm, 1200 nm, and 2409 nm are propagating along the z-axis. Without polarizer the SHG of 1200 nm and the SFG of 800 nm and 2409 nm are emitted, but no SFG of 800 nm and 1200 nm can be observed, which are perpendicular polarized to each other (Fig. 6(a)). In the other pictures a polarizer has been placed behind the parametric amplifier and was rotated from 0 ° over 45 ° to 90 °. At 0 ° just the signal wave at 1200 nm is transmitted and generates a second harmonic wave at 600 nm (Fig. 6(b)). At 45 ° all three waves are polarized parallel to each other and 45 ° with respect to the x-axis. Now, a second ring with a wavelength of 480 nm appears above the 600 nm ring (Fig. 6(c)). At 90 ° the signal wave is suppressed and only the pump wave at 800 nm and the idler wave at 2409 nm, which are polarized parallel to each other, are transmitted. A ring with a wavelength of 600 nm (SFG of 800 nm and 2409 nm) can be observed at a smaller angle than the SHG ring in the left picture (Fig. 6(d)).

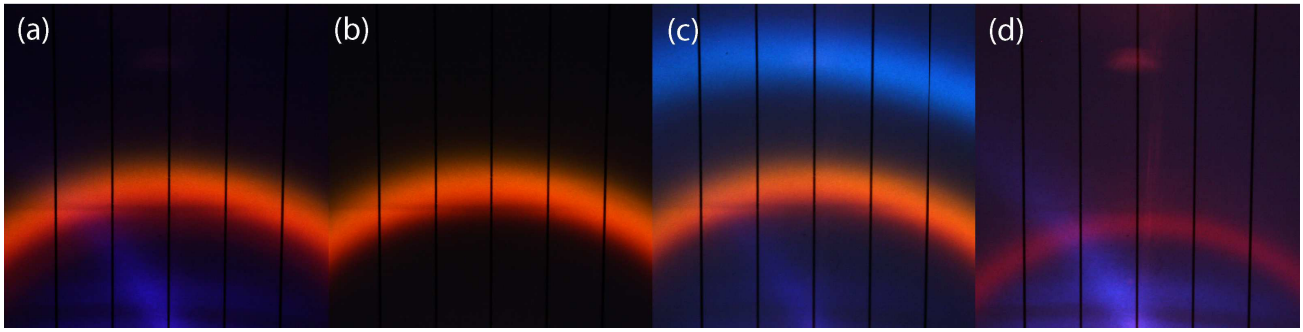

Figure 6. (Color online) SFG for different polarizations of the fundamental waves with the wavelengths 800 nm, 1200 nm, and 2409 nm. (a) without polarizer: 600 nm rings (SHG of 1200 nm, and SFG of 800 nm and 2409 nm); (b) polarizer at 0 °: 600 nm ring (SHG of 1200 nm); (c) polarizer at 45 °: 600 nm rings (SHG of 1200 nm, and SFG of 800 nm and 2409 nm), 480 nm ring (SFG of 800 nm and 1200 nm); (d) polarizer at 90 °: 600 nm ring (SFG of 800 nm and 2409 nm).

Although all fundamental waves are ordinarily polarized, the effective nonlinear polarization $P^{(2)}$ differs for different polarizations of the fundamental waves. For sum-frequency mixing in SBN the nonlinear polarization has the following form:

$$\begin{pmatrix} P_x^{(2)}(\omega_1+\omega_2) \\ P_y^{(2)}(\omega_1+\omega_2) \\ P_z^{(2)}(\omega_1+\omega_2) \end{pmatrix} = 4\epsilon_0 \begin{pmatrix} 0 & 0 & 0 & 0 & d_{15} & 0 \\ 0 & 0 & 0 & d_{24} & 0 & 0 \\ d_{31} & d_{32} & d_{33} & 0 & 0 & 0 \end{pmatrix} \times \begin{pmatrix} E_x(\omega_1)E_x(\omega_2) \\ E_y(\omega_1)E_y(\omega_2) \\ E_z(\omega_1)E_z(\omega_2) \\ E_y(\omega_1)E_z(\omega_2)+E_z(\omega_1)E_y(\omega_2) \\ E_x(\omega_1)E_z(\omega_2)+E_z(\omega_1)E_x(\omega_2) \\ E_x(\omega_1)E_y(\omega_2)+E_y(\omega_1)E_x(\omega_2) \end{pmatrix}, \tag{2}$$

with the nonlinear optically tensor d and the permittivity of free space ϵ_0. As the fundamental waves propagate along the z-axis ($E_z(\omega_1) = E_z(\omega_2) = 0$) the effective nonlinear polarization for conical SFG has the following form:

$$P_z^{(2)}(\omega_1+\omega_2) = 4\epsilon_0 d_{31}(E_x(\omega_1)E_x(\omega_2) + E_y(\omega_1)E_y(\omega_2)), \tag{3}$$

with $d_{31} = d_{32}$. A conical sum-frequency wave is only emitted if the fundamental waves have a common polarization component either along the x- or along the y-axis. Now, with the effective nonlinear polarization of Eq. 3 the results of Fig. 6 can be understood. In Fig. 6(a) the SHG of 1200 nm and the SFG of 800 nm and 2409 nm are emitted, while bot waves have the same wavelength of 600 nm. In Fig. 6(b) only one wave is frequency-doubled, because the other waves were suppressed by the polarizer. In Fig. 6(c) all waves are polarized

parallel to each other and all SFG and SHG processes are possible: SHG of 1200 nm (600 nm), SFG of 800 nm and 1200 nm (480 nm), and SFG of 800 nm and 2409 nm (600 nm). The 400 nm ring (SHG of 800 nm) experiences total internal reflection (see last section). In Fig. 6(d) the 1200 nm wave is suppressed by the polarizer and only the 600 nm ring is emitted (SFG of 800 nm and 2409 nm). The two different 600 nm second-harmonic and sum-frequency rings have different cone angles as expected by the phase matching condition (Eq. 1) and the measurements of the cone angles (Fig. 5). The angles for the SHG and SFG processes are $\Theta_{\mathrm{SHG}} = 37.3\,^\circ$ and $\Theta_{\mathrm{SFG}} = 33.3\,^\circ$, respectively.

5. SPECTRAL PULSE BROADENING

If a fs laser pulse with an energy in the μJ regime is focused into the SBN crystal the width of the SHG intensity pattern broadens as can be seen in Fig. 7. In this case the second-harmonic ring has a width of about $\Delta\Theta = 9\,^\circ$ and the total ring is extended from $33\,^\circ$ to $42\,^\circ$. The covered spectrum is 550 nm – 650 nm. This spectral pulse

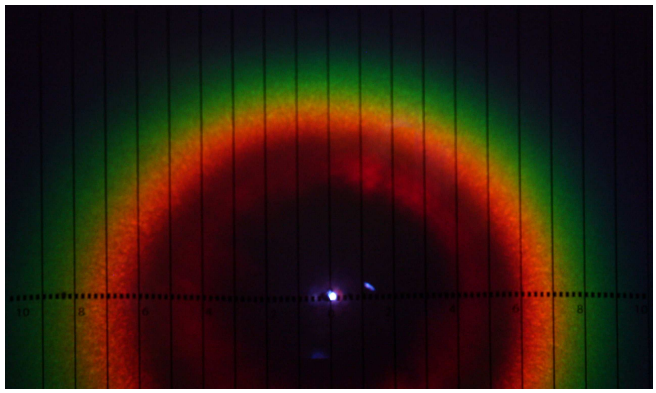

Figure 7. (Color online) Conical SHG of a focused 1200 nm pulse.

broadening is attributed to a self-phase modulation due to the Kerr effect. To study this process in detail we have measured the SHG spectrum of a collimated 1200 nm pulse on the ring for different input pulse energies. The spectral SHG width (FWHM) increases linearly with increasing pulse energy (Fig. 8(a)). This behavior can

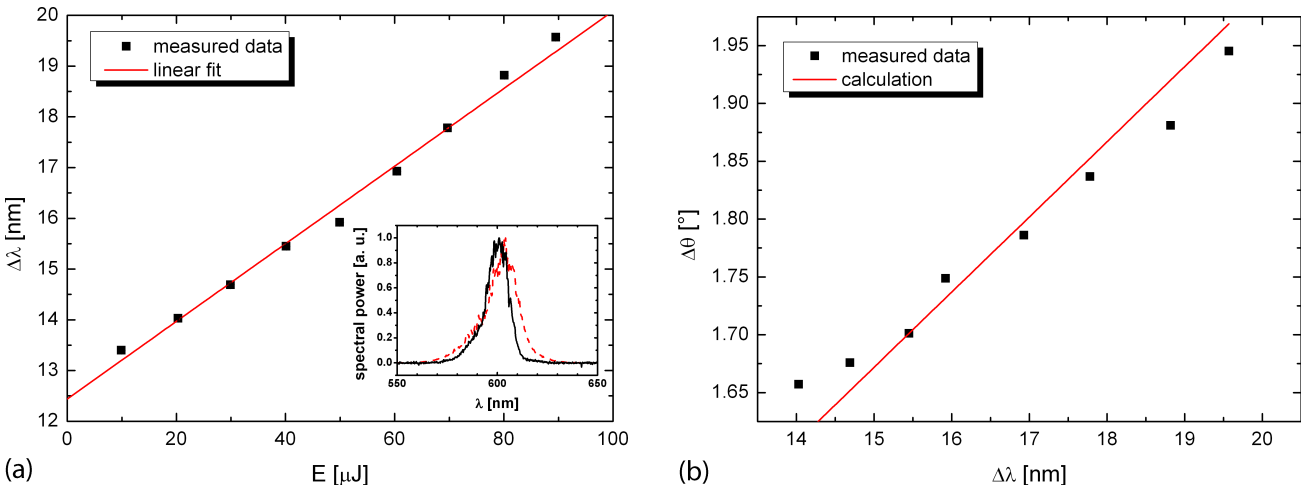

Figure 8. Spectral broadening of 600 nm pulses (SHG of 1200 nm). (a): the spectral width $\Delta\lambda$ increases linearly with increasing pulse energy (inset: pulse spectrum for two different pulse energies); (b): the angular width increases linearly with increasing spectral width $\Delta\lambda$.

be explained by a broadening of the 1200 nm pulse due to self-phase modulation. When the Kerr nonlinearity is stronger than the group velocity dispersion, it is expected that the spectral width of the 1200 nm pulse increases

linearly with increasing intensity. Therefore, the same dependence is expected for the SHG pulse. However, a cross-phase modulation between the 1200 nm and 600 nm pulse might also lead to an additional broadening of the SHG pulse. The intensity-independent spectral width at 600 nm is $\Delta\lambda_0(600\,\mathrm{nm}) = 12.5\,\mathrm{nm}$. Assuming a complete mapping of the infrared to the visible spectrum,[7] the spectral width of the 1200 nm pulse should be $\Delta\lambda_0(1200\,\mathrm{nm}) = 2\Delta\lambda_0(600\,\mathrm{nm}) = 25\,\mathrm{nm}$. This would result in a time-bandwidth-product for the 1200 nm pulse of $\Delta\nu \cdot \Delta\tau = 0.41$ for $\Delta\tau = 80\,\mathrm{fs}$, which fits well to a Fourier limited 1200 nm pulse. The measured angular width of the SHG ring also increases with increasing pulse energy as can be seen in Fig. 8(b). For spectral narrow pulses we expect a minimum width $\Delta\Theta_0$, which is independent of the spectral width. If the pulse broadening is not too large ($\Delta\lambda < 100\,\mathrm{nm}$) the cone angle at a given wavelength will depend approximately linearly on the wavelength change. The line in Fig. 8(b) is a linear fit according to:

$$\Delta\Theta(\Delta\lambda) = \Delta\Theta_0 + \delta\Theta(\Delta\lambda) = \Delta\Theta_0 + m \cdot \Delta\lambda\,, \tag{4}$$

where the slope m is the calculated broadening factor $m = 0.07\ ^\circ/\mathrm{nm}$ at 600 nm (Eq. 1) and the minimal angular width $\Delta\Theta_0$ is a free parameter. The line fits well to the experimental data. By measuring the angular width of the ring it is therefore possible to determine the spectral pulse broadening. The measurement of the absolute spectral pulse width is limited by the value of Θ_0. The minimum angular width Θ_0 should depend on geometrical parameters like the spatial pulse width and the propagation length. It can also be assumed that the domain length along the c-axis has an impact on the angular width of the SHG intensity profile.[9] We are currently working on the experimental verification of the influence of the order of the domains on the SHG properties by designing different ferroelectric domain gratings in SBN.[26–29]

6. CONCLUSION

We have studied experimentally the process of noncollinear sum-frequency generation of femtosecond laser pulses in strontium barium niobate with a random domain structure. When pulses of different frequency are propagating along the c-axis, new second-harmonic and sum-frequency waves are emitted on a cone. The cone angles of the sum-frequency waves have been measured for the first time over a large wavelength range from $460\,\mathrm{nm} - 630\,\mathrm{nm}$ and the results agree very well with theory. By changing the polarization of the fundamental waves we are able to generate different colors on the sum-frequency ring. The propagation of femtosecond laser pulses with energies in the μJ range lead to strong self-phase modulation resulting in a spectral pulse broadening. The spectral broadening can be determined by measuring the angular width of the second-harmonic ring. This makes conical second-harmonic and sum-frequency generation an ideal tool to study nonlinear pulse propagation and to examine the influence of the domain structure on the parametric processes.

ACKNOWLEDGMENTS

We gratefully acknowledge the support of ALTECHNA Co. Ltd., Konstitucijos ave. 23C-604, LT-08105, Vilnius, Lithuania, who have supplied the SBN crystal.

REFERENCES

[1] Fejer, M. M., Magel, G. A., Jundt, D. H., and Byer, R. L., "Quasi-phase-matched second harmonic generation: Tuning and tolerances," *IEEE J. Quantum. Electron.* **28**, 2631 (1992).

[2] Berger, V., "Nonlinear photonic crystals," *Phys. Rev. Lett.* **81**, 4136 (1998).

[3] Baudrier-Raybaut, M., Haidar, R., Kupecek, P., Lemasson, P., and Rosencher, E., "Random quasi-phase-matching in bulk polycrystalline isotropic nonlinear materials," *Nature* **432**, 374 (2004).

[4] Molina, P., Álvarez García, S., Ramírez, M. O., García-Solé, J., Bausá, L. E., Zhang, H., Gao, W., Wang, J., and Jiang, M., "Nonlinear prism based on the natural ferroelectric domain structure in calcium barium niobate," *Appl. Phys. Lett.* **94**, 071111 (2009).

[5] Aleksandrovsky, A. S., Vyunishev, A. M., Shakhura, I. E., Zaitsev, A. I., and Zamkov, A. V., "Random quasi-phase-matching in a nonlinear photonic crystal structure of strontium tetraborate," *Phys. Rev. E* **78**, 031802(R) (2008).

[6] Kawai, S., Ogawa, T., Lee, H. S., DeMattei, R. C., and Feigelson, R. S., "Second-harmonic generation from needlelike ferroelectric domains in $Sr_{0.6}Ba_{0.4}Nd_2O_6$ single crystals," *Appl. Phys. Lett.* **73**, 768 (1998).

[7] Fischer, R., Saltiel, S. M., Neshev, D. N., Krolikowski, W., and Kivshar, Y. S., "Broadband femtosecond frequency doubling in random media," *Appl. Phys. Lett.* **89**, 191105 (2006).

[8] Tunyagi, A. R., Ulex, M., and Betzler, K., "Noncollinear optical frequency doubling in strontium barium niobate," *Phys. Rev. Lett.* **90**, 243901 (2003).

[9] Kuznetsov, K. A., Kitaeva, G. K., Shevlyugaand, A. V., Ivleva, L. I., and Volk, T. R., "Second harmonic generation in a strontium barium niobate crystal with a random domain structure," *JETP Letters* **87**, 98 (2008).

[10] Molina, P., de la O Ramírez, M., and Bausá, L. E., "Strontium barium niobate as a multifunctional two-dimensional nonlinear photonic glass," *Adv. Funct. Mater.* **18**, 709 (2008).

[11] Saltiel, S. M., Neshev, D. N., Fischer, R., Krolikowski, W., Arie, A., and Kivshar, Y. S., "Spatiotemporal toroidal waves from the transverse second-harmonic generation," *Opt. Lett.* **33**, 527 (2008).

[12] Fischer, R., Neshev, D. N., Saltiel, S. M., Sukhorukov, A. A., Krolikowski, W., and Kivshar, Y. S., "Monitoring ultrashort pulses by transverse frequency doubling of counterpropagating pulses in random media," *Appl. Phys. Lett.* **91**, 031104 (2007).

[13] Trull, J., Saltiel, S., Roppo, V., Cojocaru, C., Dumay, D., Krolikowski, W., Neshev, D., Vilaseca, R., Staliunas, K., and Kivshar, Y., "Characterization of femtosecond pulses via transverse second-harmonic generation in random nonlinear media," *Appl. Phys. B* **95**, 609 (2009).

[14] Dumay, D., Saltiel, S. M., Neshev, D. N., Krolikowski, W., and Kivshar, Y. S., "Pulse measurements by randomly quasi phase matched second harmonic generation in the regime of total internal reflection," *J. Phys. B* **42**, 175403 (2009).

[15] Voelker, U. and Betzler, K., "Domain morphology from k-space spectroscopy of ferroelectric crystals," *Phys. Rev. B* **74**, 132104 (2006).

[16] Voelker, U., Heine, U., Gödecker, C., and Betzler, K., "Domain size effects in a uniaxial ferroelectric relaxor system: The case of $Sr_xBa_{1-x}Nb_2O_6$," *J. Appl. Phys.* **102**, 114112 (2007).

[17] Isakov, D. V., Belsley, M. S., Volk, T. R., and Ivleva, L. I., "Diffuse second harmonic generation under the ferroelectric switching in $Sr_{0.75}Ba_{0.25}Nb_2O_6$ crystals," *Appl. Phys. Lett.* **92**, 032904 (2008).

[18] Isakov, D. V., Volk, T. R., and Ivleva, L. I., "Investigation of ferroelectric properties of strontium barium niobate crystals by second harmonic generation technique," *Physics of the Solid State* **51**, 2334 (2009).

[19] Volk, T., Isakov, D., Belsley, M. S., and Ivleva, L., "Switching kinetics of a relaxor ferroelectric $Sr_{0.75}Ba_{0.25}Nb_2O_6$ observed by the second harmonic generation method," *Phys. Status Solidi A* **2**, 321 (2009).

[20] Wang, W., Roppo, V., Kalinowski, K., Kong, Y., Neshev, D. N., Cojocaru, C., Trull, J., Vilaseca, R., Staliunas, K., Krolikowski, W., Saltiel, S. M., and Kivshar, Y., "Third-harmonic generation via broadband cascading in disordered quadratic nonlinear media," *Optics Express* **17**, 20117 (2009).

[21] Romero, J. J., Jaque, D., Sole, J. G., and Kaminskii, A. A., "Diffuse multiself-frequency conversion processes in the blue and green by quasicylindrical ferroelectric domains in Nd^{3+}:$Sr_{0.6}Ba_{0.4}(NbO_3)_2$ laser crystal," *Appl. Phys. Lett.* **78**, 1961 (2001).

[22] Romero, J. J., Jaque, D., Sole, J. G., and Kaminskii, A. A., "Simultaneous generation of coherent light in the three fundamental colors by quasicylindrical ferroelectric domains in $Sr_{0.6}Ba_{0.4}(NbO_3)_2$," *Appl. Phys. Lett.* **81**, 4106 (2002).

[23] Woike, T., Granzow, T., Dörfler, U., Poetsch, C., Wöhlecke, M., and Pankrath, R., "Refractive indices of congruently melting $Sr_{0.61}Ba_{0.39}Nb_2O_6$," *phys. stat. sol. (a)* **186**, R13 (2001).

[24] Trull, J., Cojocaru, C., Fischer, R., Saltiel, S. M., Staliunas, K., Herrero, R., Vilaseca, R., Neshev, D. N., Krolikowski, W., and Kivshar, Y. S., "Second-harmonic parametric scattering in ferroelectric crystals with disordered nonlinear domain structures," *Optics Express* **15**, 15868 (2007).

[25] Fischer, R., SaItiel, S. M., Neshev, D. N., Krolikowski, W., Dreischuh, A., and Kivshar, Y. S., "Frequency doubling in SBN crystals with random ferroelectric domains in the thermal focusing regime," *Proc. of SPIE* **6604**, 6604F–1 (2007).

[26] Horowitz, M., Bekker, A., and Fischer, B., "Broadband second-harmonic generation in $Sr_xBa_{1x}Nb_2O_6$ by spread spectrum phase matching with controllable domain gratings," *Appl. Phys. Lett.* **62**(21), 2619 (1993). HBF1993.121.

[27] Horowitz, M., Bekker, A., and Fischer, B., "Simultaneous generation of sum, difference, and harmonics of two laser frequencies by spread spectrum phase matching," *Appl. Phys. Lett.* **65**, 679 (1994).

[28] Fischer, B. and Horowitz, M., "Controllable narrow band and broadband second-harmonic generation by tailored quasiphase matching with domain gratings," *Appl. Phys. Lett.* **64**, 1756–1758 (1994).

[29] Kahmann, F., Pankrath, R., and Rupp, R., "Photoassisted generation of ferroelectric domain gratings in SBN," *Opt. Commun.* **107**, 6 (1994).